Received 25 October 2022; revised 25 November 2022; accepted 2 February 2023. Date of publication 7 February 2023; date of current version 22 February 2023.
The review of this article was arranged by Editor Z. Zhang.

*Digital Object Identifier 10.1109/JEDS.2023.3243056*

# A Flexible Printed Circuit Board-Based ZnO Enzymatic Uric Acid Potentiometric Biosensor Measurement and Characterization

**PO-HUI YANG (Member, IEEE), CHE-TSUNG CHAN, AND YING-SHENG CHANG**

Graduate School of Electronic Engineering, National Yunlin University of Science and Technology, Douliou 64002, Taiwan

CORRESPONDING AUTHOR: P.-H. YANG (e-mail: phyang@yuntech.edu.tw)

This work was supported by the National of Science and Technology Council, China, under Contract NSTC 111-2221-E-224-058.

**ABSTRACT** This study prepared an enzymatic potentiometric uric acid sensor based on zinc oxide (ZnO) and uricase. Also, we develop a potentiometric differential measurement system. We applied Nafion, APTES, and glutaraldehyde to immobilize the enzyme and increase sensitivity to prevent enzyme leakage. Thus, the uric acid sensor was integrated into FPCB which could provide flexibility to the sensor. In the uric acid concentration range of 2 mg/dL-10 mg/dL, we analyzed the characteristics of sensors with the voltage-time measurement system, measuring the average sensitivity, linearity, response time, limit of detection (LOD), and interference effects. The modification of Nafion and uricase improved the performance of the uric acid sensor.

**INDEX TERMS** Zinc oxide (ZnO), uric acid (UA), biosensor, enzymatic, instrumentation amplifier (INA).

## I. INTRODUCTION

Uric acid (UA) is the final metabolite of purines in the human body. Uric acid is one of the indicators of obesity, high blood pressure, and hyperlipidemia in the human body [1]. The main reasons for excessive uric acid production are often drinking too little water and doing anaerobic exercise without massage afterward. The innate constitution is easy to further metabolize the ingested purines into excrement that can be excreted from the kidneys through the urine during the metabolic process. Reptiles and birds convert metabolic waste ammonia into uric acid for excretion. These substances eventually form excess uric acid, which then flows to connective tissue through the blood, where it is stored as crystals and causes gout. Therefore, monitoring the concentration of uric acid in human blood and urine can effectively predict gout symptoms [2].

In 1906, the development of medical sensors begins. Max Cremer used a glass tube to detect hydrogen ions [3], and was used as a simple sensor by observing the foam generation. It was also later used as the basis for developing glass electrodes. Soon after, Leland in the United States Clark proposed the first biomedical sensor made of oxygen-sensing electrodes in 1956 [4] and soon launched an enzyme-based biomedical sensor for glucose. The detection of uric acid in urine and blood includes non-enzymatic and enzymatic detection. The detection utilizes the combination of phosphate-buffered saline (PBS) and UA powder to form a solution to stimulate UA's normal concentration in the human body [5]. The reactant in the sensor will have a catalytic reaction with uric acid and has a linear relationship with the concentration of uric acid in the solution to be tested. Non-enzymatic sensors are less susceptible to environmental factors and have a longer shelf life [6], [7], but have poor selectivity and are susceptible to other interferences. Enzymatic detection uses enzymes that are easy to catalyze uric acid. The enzymatic sensor has a higher average sensitivity. However, enzymes are susceptible to environmental factors and have a limited shelf life [5]. John and Bulger used the first uricase enzyme to detect uric acid in 1941 [8], to analyze the among of uric acid catalyzed by uricase. Also, there is a difference in methods to determine uric acid, such as optic fiber [9], [10], [11], SERS [12], optic SPR [13], and fluorescent [14] methods that have been used in the uric acid sensor. However, these methods are complicated

and expensive. Therefore, electrochemical was a simple and easy way to cooperate with enzyme sensors. Uric acid interacts with uricase in solution to produce hydrogen peroxide ($H_2O_2$), carbon dioxide ($CO_2$), and allantoin. Meanwhile, hydrogen ion ($H^+$) was decomposed from $H_2O_2$ which could be detected by ion-sensitive material. As a result, a medium such as an ion-sensitive membrane would need to conduct the potential between the electrode and uricase. Zinc oxide (ZnO) is widely used in pH sensors [15] and various biosensors. It has various applications due to its unique chemical properties such as wide band gap, non-toxicity, high excitation binding energy, and biocompatibility. Hence, the ZnO thin film would be suitable for an ion-sensitive medium.

Various substrates can be applied to the electrochemical sensor, such as PET, silicon, and glass [16]. In this work, polyimide (PI) was applied to the sensor's substrate due to being commonly used in the flexible printed circuit board (FPCB) standard process. Also, polyimide is attributed to excellent flexibility and high mechanical strength. On top of PI, copper wire and immersion gold can provide good electrical conductivity characteristics and chemical stability [17]. Furthermore, the FPCB has the potential to integrate with electronic circuits such as analog readout frontend and power management circuits for battery devices that can dramatically reduce the device's size.

In electrochemical measurement, amperometry was commonly used to analyze sensor performance. Meanwhile, the three-electrode system is a mature way in sensory. However, amperometry needs a complex circuit to form a measurement system that is hard to integrate sensor and measurement system. Furthermore, potentiometric measurement only needs a few components to build a system and is easy to integrate with the sensor. Hence, this study used potentiometric measurement in the electrochemical sensor characterization.

## II. EXPERIMENTAL

### A. MATERIALS

The ZnO targets (99%) were purchased from Ultimate Materials Technology Co., Ltd. (Taiwan). The substrate of the pH sensor was FPCB, which was a contract manufactured by Rui Xing Circuit Co., Ltd. (China). The uric acid powder, uricase (from Arthrobacter Globiformis, 15-30 unit/mg), (3-aminopropyl) tri-ethoxysilane ($\gamma$-APTES), and glutaraldehyde were purchased from Sigma-Aldrich Co. (USA). Eventually, the phosphate-buffered saline (PBS, pH7) used to prepare the uric acid solution was purchased from AppliChem GmbH Crop (Darmstadt, Germany).

### B. FABRICATION OF THE URIC ACID SENSING FILM

Fig. 1 shows the preparation process of working electrodes from (A) to (E) for functional working electrodes in UA detection. First, start with step (A), the FPCB substrate was cleaned with distilled (DI) water, acetone, and ethanol. Next, step (B) used the radio frequency (RF) sputtering system to deposit ZnO thin film on the working electrode. Table 1 shows the ZnO film sputtering parameter [18], deposited with RF power 60 W and deposition pressure 3 mTorr to make sure the purity of the process. Also, argon and oxygen were led into the chamber at a flow ratio was 9:1 (sccm) and deposited for 15 minutes to achieve the expected thickness.

**TABLE 1. ZnO thin film sputtering parameters.**

| Film thickness | Gas flow ratio (Ar: $O_2$) | RF power | Deposition pressure | Deposition time |
|---|---|---|---|---|
| 74.8 nm | 9:1(sccm) | 60W | 3 mTorr | 15 minutes |

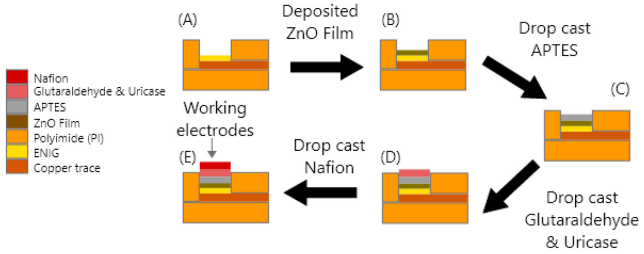


**FIGURE 1. Preparation of the uric acid sensor working electrode.**

To immobilize the uricase onto the ZnO thin film, in step (C), the $\gamma$-APTES (1% wt) diluted with buffer solution and drop cast 2 $\mu$L onto the ZnO thin film twice, which could protect the ZnO film and functionalize to cooperate with organic materials. Therefore, in step (D), the 2 $\mu$L of glutaraldehyde was modified onto the $\gamma$-APTES with the drop cast technique. Before casting the uricase onto the electrode, the 6.3 mg of uricase (15 unit/mg) was mixed with a 2.5 mL buffer solution (pH 7). Meanwhile, prepare glutaraldehyde solution (1 wt%) and mix uricase: glutaraldehyde with a 6:4 ratio to apply cross-linking method [19]. Then, drop cast 2 $\mu$L uricase: glutaraldehyde cross-linking solution to the glutaraldehyde layer. Glutaraldehyde had well binding force between the biocatalyst such as the enzyme. Eventually, in step (E), 2 $\mu$L of Nafion (5 wt%) was modified [20] onto the working electrode to prevent possible uricase leakage [21], [22].

### C. SENSOR STRUCTURE AND MEASUREMENT SYSTEM

Fig. 2 (a) illustrates the cross-section structure of the UA biosensor. The substrate is based on the standard process of the single-layer flexible printed circuit board (FPCB). Using polyimide (PI) as the cover film has decent flexibility and temperature resistance. Also, rolled and annealed cooper was applied in the copper wire can provide mechanical strength in bend conditions [23]. Furthermore, electroless nickel immersion gold (ENIG), known as the chemical Ni/Au, can prevent copper wire oxidation and improve the solderability of copper contact. Lastly, a stiffener is adhesive under the connector to enhance sensor connection stability. Fig. 2 (b) illustrates the uric acid sensor structure diagram. The sensor array consists of two working electrodes, reference electrodes, and a ground electrode. The working electrode diameter is 2 mm,

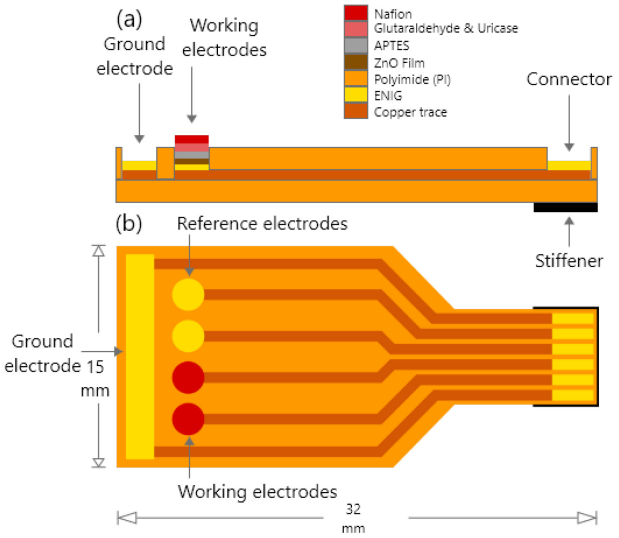


**FIGURE 2.** Uric acid sensor (a) cross-section (b) plan view.

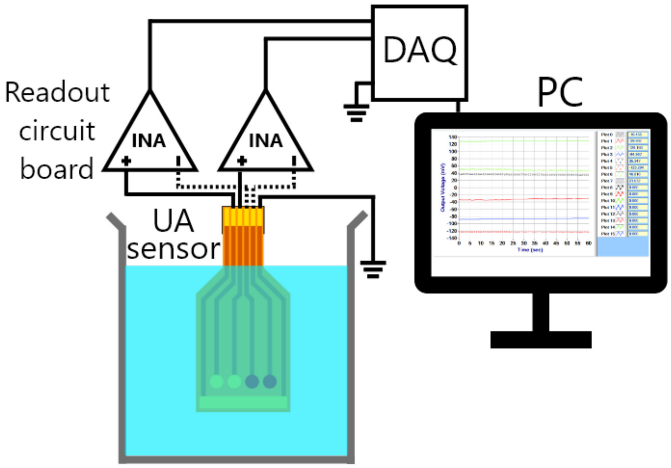


**FIGURE 3.** The schematic of the measurement system.

and the fabricated Nafion/uricase/APTES/ZnO structure is on top of the ENIG and copper wire substrate.

The voltage-time (V-T) measurement system measure the FPCB UA sensor voltage response, which was demonstrated in Fig. 3 shows the sensor connection schematic. The FPCB sensor includes working electrodes, reference electrodes, and the ground channel connected through the FPCB connector. The connector is connected to a readout circuit consisting of an instrumentation amplifier (INA) board. Also, the INA readout circuit board uses the LT1167 as an INA for each channel and is powered by the wall power transformer. Furthermore, the ground electrode is connected to the ground to provide a current path to input that creates an input bias current return path to prevent input common mode saturation [24]. Also, the UA sensor total measurement setup can be present in Fig. 4. Then, the circuit board output terminal is connected to the data acquisition (DAQ) instrument, and the model of the DAQ is National Instruments

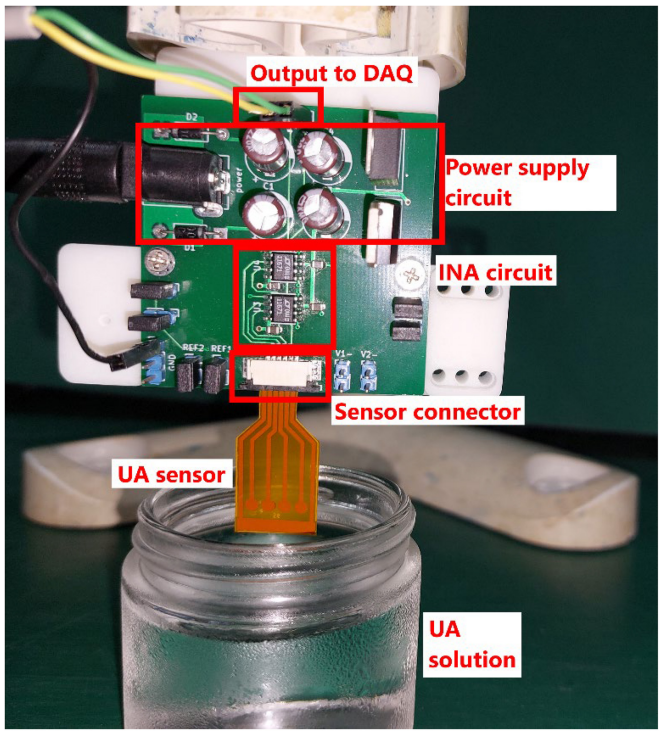


**FIGURE 4.** UA sensor and measurement system connection setup.

(USA) USB-6201. It can convert analog sensing signals to digital signals through internal 16 bits ADC. Eventually, the data on response voltages are accessed via LabVIEW software [25].

## III. RESULT AND DISCUSSION

### A. ANALYSIS OF THE ZINC OXIDE CHARACTERISTIC

In this study, we used Field-emission scanning electron microscopy (FE-SEM) to analyze the film thickness and surface morphology. In this analysis setup, the ZnO film was RF-sputtered on a Si substrate. In the ZnO cross-section view, shown in Fig. 5(a), many columnar grains can be observed and grows evenly. That result leads to ZnO having a smooth and flat surface [26]. Also, the average thickness of 74.8 nm can be measured. Fig. 5(b) shows the top perspective of the ZnO film. The columnar grains grow in high density. The average particle size was calculated in Fig. 5(b) 10 sampling points have 31.2 nm.

X-ray photoelectron spectroscopy (XPS) was used to analyze the ZnO film chemical composition and the electronic state of the atoms within a material. The C 1s (283.8 eV) spectrum was used as calibration of binding energy positions for XPS spectra [27]. Fig. 6 (a) shows the Zn 2p spectrum. The binding energy has two peaks at 1021.1 eV representing Zn $2p_{3/2}$ and 1044.3 eV representing Zn $2p_{1/2}$. The Zn $2p_{3/2}$peak was present as the metallic zinc in stoichiometric ZnO and the Zn $2p_{1/2}$ peak was present as $Zn^{2+}$ in the hypoxic region. The difference of 23.2 eV between Zn $2p_{1/2}$ and Zn $2p_{3/2}$ represents the binding energy difference

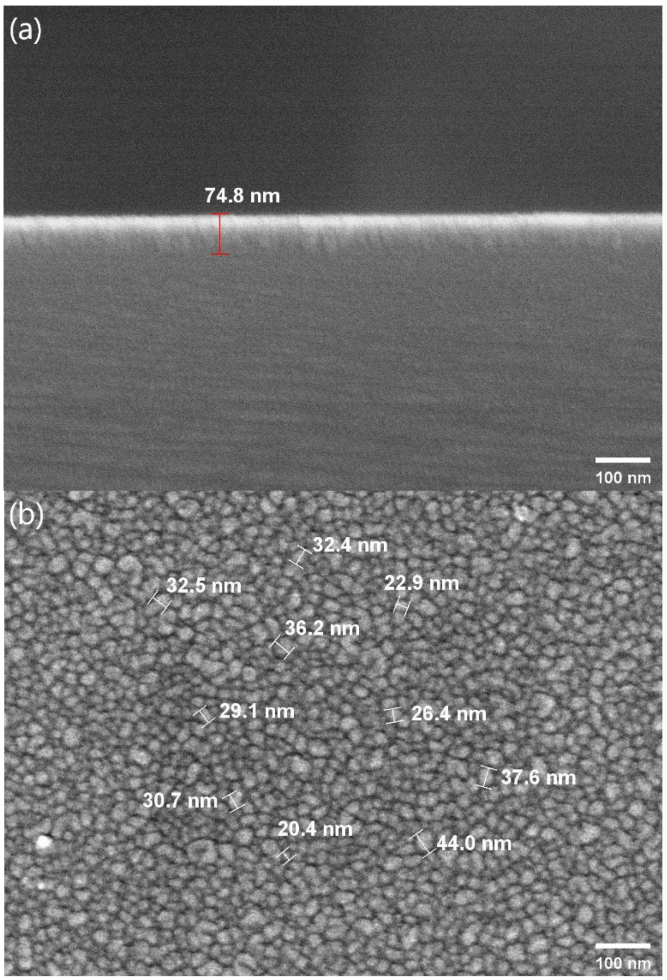


**FIGURE 5.** The zinc oxide morphology. (a) cross-section view (b) top view.

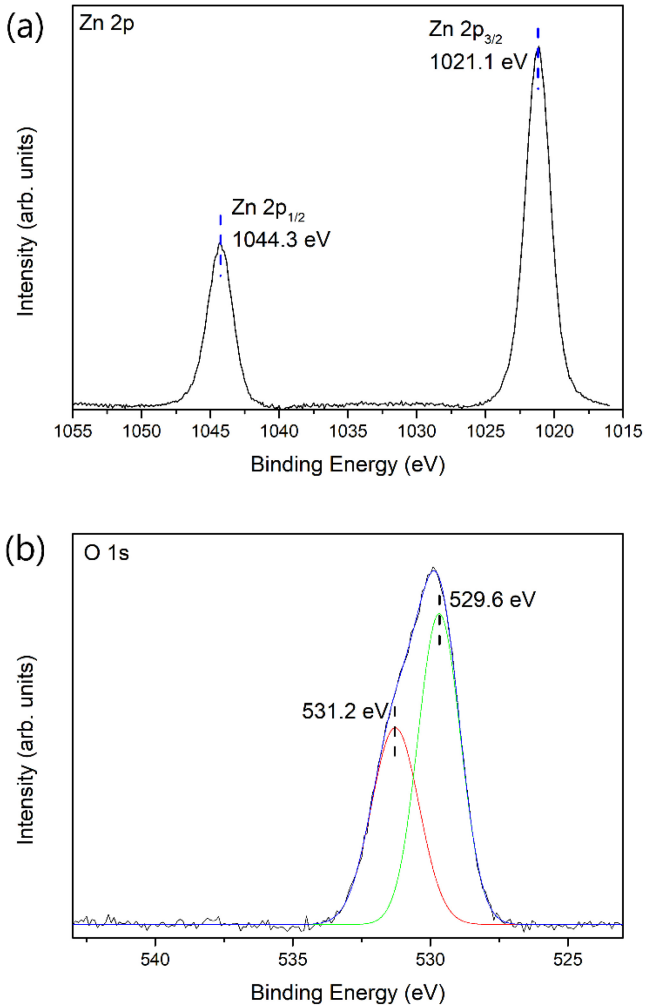


**FIGURE 6.** The zinc oxide thin film high-resolution XPS spectrum. (a) Zn 2p spectrum and (b) O 1s spectrum.

between these two peaks proving that zinc exists in the $Zn^{2+}$ oxidation state [28].

Fig. 6 (b) shows the O 1s binding energy graph. Two singlet peaks fit in the gauss method were 529.6 eV and 531.2 eV [29]. The first peak, 529.6 eV, was associated to the $O^{2-}$ ion [29] in the ZnO structure. The second peak, 531.2 eV, was due to the contribution of the $O^{2-}$ ion in the oxygen defect regions in the ZnO film [29].

To analyze ZnO film chemical composition and oxidation state. The relative sensitivity was used to measure and calculated the peaks' integral area. Adjust the scale to a different element. In that case, Zn $2p_{3/2}$, Zn $2p_{1/2}$, and O 1s have calculated the peaks' integral area [29]. After that, divide the relative sensitivity value of each element. In this case, the relative sensitivity factors are 2.768 of Zn $2p_{3/2}$, 1.384 of Zn $2p_{1/2}$, and 0.733 of O 1s. The zinc to oxygen (Zn/O) atomic concentration ratio can be calculated depending on different relative sensitivity factors. The proportion of oxygen atoms in ZnO film is about 47%, and the proportion of zinc atoms is 53%. The ratio of zinc to oxygen was 1.12 which shows that the ZnO thin film was successfully fabricated.

### B. REACTION MECHANISM BETWEEN THE URICASE AND THE URIC ACID

As equation (1) shows, the uricase catalyzes uric acid ($C_5H_4N_4O_3$) and water into allantoin ($C_5H_6N_4O_3$), carbon dioxide ($CO_2$), and hydrogen peroxide ($H_2O_2$). Automatically, as equation (2) shows, $H_2O_2$ decomposed into a hydrogen ion ($H^+$), oxygen ($O_2$), and an electron $e^-$) [30].

$$\text{Uric Acid} + H_2O + O_2 \xrightarrow{\text{Uricase}} \text{Allantoin} + CO_2 + H_2O_2 \quad (1)$$

$$H_2O_2 \rightarrow O_2 + 2e^- + 2H^+ \quad (2)$$

According to previous research [31], the response voltage changes in different $H^+$ concentration and relate to different UA concentration. Also, the response voltage determined by the oxidation reaction shows in equation (3), equation (4), and Nernst [31] equation (5).

$$Zn(OH)_{2(s)} + H^+_{(aq)} = ZnOH^+_{(aq)} + H_2O \quad (3)$$

$$ZnO_{2H^+_{(aq)}} + H^+_{(aq)} = Zn(OH)_{2(s)} \quad (4)$$

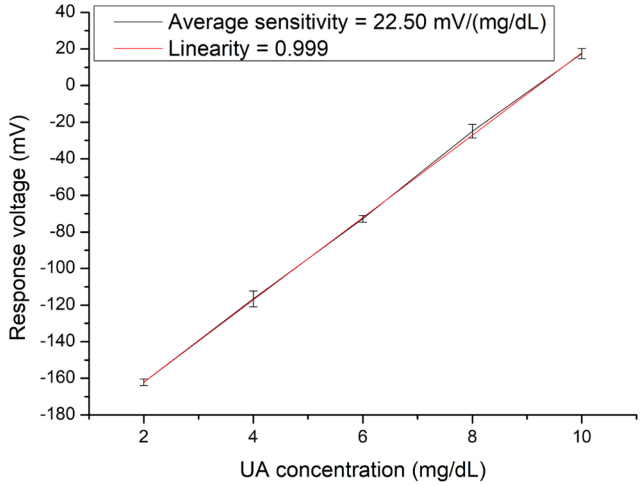


**FIGURE 7.** The average sensitivity and linearity of the UA sensor.

$$\mathrm{E} = \mathrm{E}^0 - \frac{RT}{F} \ln \frac{[\mathrm{ZnOH}]}{[\mathrm{ZnO}][\mathrm{H}^+]} \tag{5}$$

where $\mathrm{E}^0$ represents the reference electrode potential, R represents the gas constant, F represents Faraday's constant, and T represents the absolute temperature.

### C. AVERAGE SENSITIVITY OF THE URIC ACID SENSOR

Fig. 7 shows the FPCB UA sensor is measure UA in 2 mg/dL, 4 mg/dL, 6 mg/dL, 8 mg/dL, 10 mg/dL concentrations in V-T method. The average sensitivity is 22.50 mV/(mg/dL), and the linearity is 0.999. The average sensitivity formula [32] can be stated as formula (6).

$$S_0 = \Delta V / R \tag{6}$$

where $S_0$ represents the average sensitivity, $\Delta V$ represents the change amplitude of the sensor signal, and $R$ represents the concentration range of the measurement.

### D. REPRODUCIBILITY

Reproducibility is an important indicator representing the sensor's stability and reliability [32]. Meanwhile, indicate the accuracy and precision of the electron devices. In this experiment, we immersed the Nafion/uricase/ZnO FPCB uric acid (UA) sensor in 2 mg/dL, 4 mg/dL, 6 mg/dL, 8 mg/dL, and 10 mg/dL concentration UA solution. The voltage-time (V-T) measurement system was employed to measure the average sensitivity and linearity. Fig. 8 shows each sensor's average sensitivities and linearities. The relative standard deviation (RSD) represents sensor reliability [33]. The average sensitivity of the sensors is 19.48 mV/(mg/dL), and the standard deviation is 1.59 mV/(mg/dL). Therefore, the relative standard deviation (RSD) calculated is 8.2%. The RSD proved that the sensor had enough reliability in this study.

### E. RESPONSE TIME OF THE URIC ACID SENSOR

In Fig. 9, we immersed UA sensors in 50 mL pH 7 phosphate-buffered saline (PBS) solution. When the response voltage was stable, 250 $\mu$L of 6 mg/dL (0.33 mM) concentration uric acid solution was added to the solution. Then, waiting for the response voltage to be stable, we can measure the response voltage from 0% to 95% time interval [34]. Fig. 9 shows the UA sensor response time of 7 seconds.

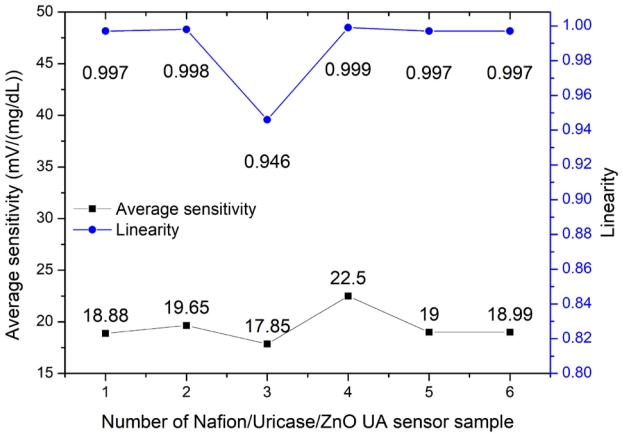


**FIGURE 8.** Uric acid sensor reproducibility.

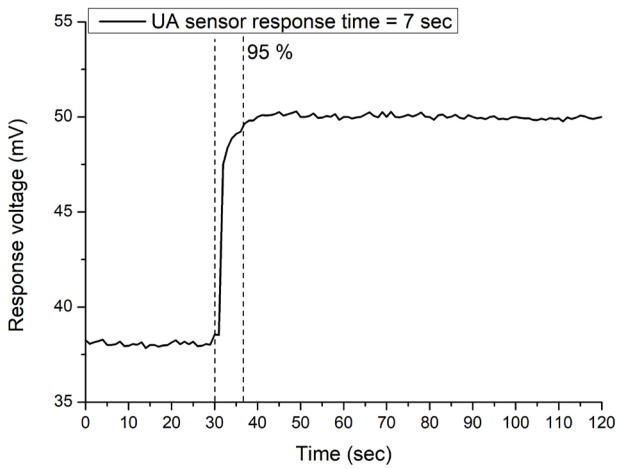


**FIGURE 9.** FPCB UA sensors response time measurement result.

### F. INTERFERENCE EFFECTS OF THE URIC ACID SENSOR

The interference effect is an important indicator in biosensors. This effect mainly presents the sensing performance when the sensor has interfered with other substances. In this experiment, the sensor was immersed in phosphate-buffered saline (pH7) 50 mL first and waited for the response voltage to become stationary. Then, 0.110 mM (2 mg/dL) uric acid (UA), 0.025 mM ascorbic acid (AA), 7.000 mM glucose (Glu), 0.400 mM fructose (Fr), 1.100 mM urea (UR), 0.150 mM dopamine (DA) and 0.330 mM (6 mg/dL) UA were sequentially added 250 $\mu$L per interference substance into the phosphate buffered saline every 30 seconds. Therefore, the voltage changes difference of each interference added could be observed. The concentration of the substances was based on the concentration range of the

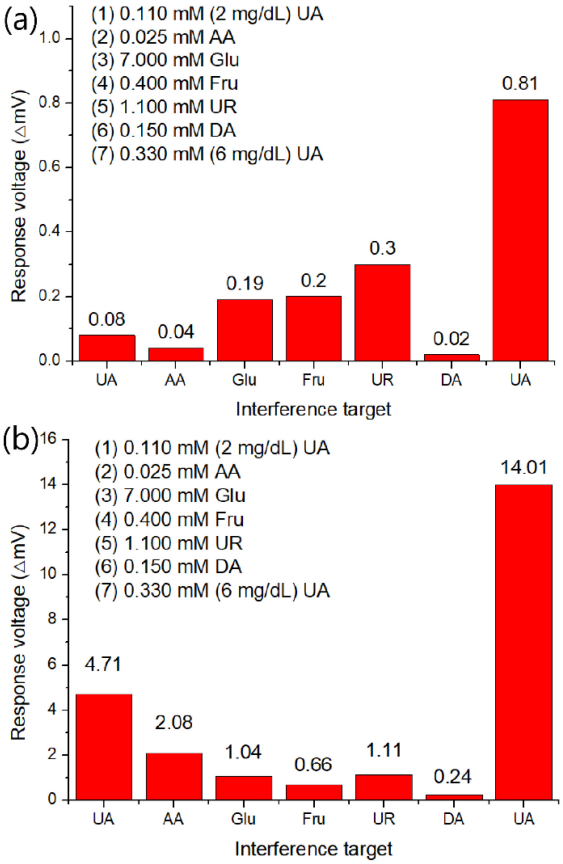


**FIGURE 10.** Uric acid sensor interference effect experiment result (a) without uricase and (b) with uricase.

human body, and the last medium concentration of uric acid was selected.

Fig. 10(a) shows the interference on the working electrodes with the bare ZnO film. As shown in Fig. 10(a), without uricase modification, the voltage response of low UA concentration 0.08 mV did not outperform Glu 0.19 mV, Fr 0.2 mV, and UR 0.3 mV voltage responses. However, Fig. 10(b) shows the interference test on the working electrodes with the Nafion/uricase/ZnO structure. Fig. 10(b) shows that Glu, Fr, AA, DA, and UR have fewer voltage response differences than UA in low concentrations of voltage response of 4.71 mV. Hence, the uricase-modified ZnO enzymatic sensor has good selectivity in UA.

### G. LOD OF THE URIC ACID SENSOR

The limit of detection (LOD) represents a specification that indicates the lowest measurement concentration that can detect. In that case, we use the 3-sigma method [35] to calculate LOD and the formula shown in formula (7). The FPCB-based Nafion/Uricase/ZnO uric acid sensing windows were measured, and the LOD was calculated by the 3-sigma method. When average sensitivity was 22.5 mV/(mg/dL). The response voltage of the pure pH 7.0 BS solution was −30.4 mV, the standard deviation of solution response voltage $\sigma$ was 0.944 mV, and $S_0$ was the average sensitivity of

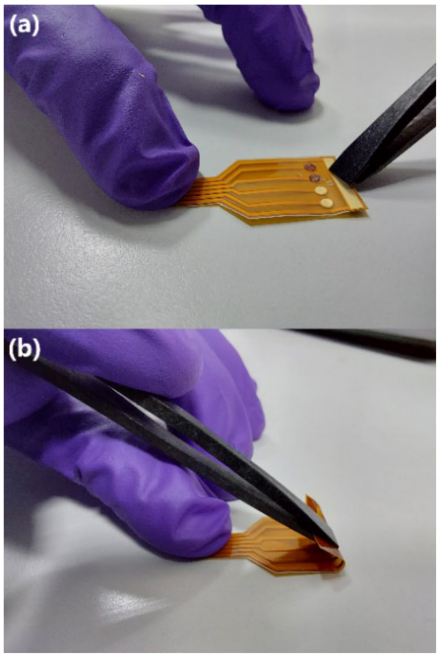


**FIGURE 11.** UA sensor flexible test method demonstration when the sensor is on the (a) flat state (b) curve state.

the sensor. Hence, The $C_{LOD}$ was calculated as 0.12 mg/dL (∼7.14 $\mu$M).

$$C_{LOD} = \frac{3\sigma}{S_0} \tag{7}$$

where the $C_{LOD}$ is the LOD of the concentration, $\sigma$ is the standard deviation of response voltage when the pure PBS solution was measured, and $S_0$ is the sensitivity.

### H. FLEXIBILITY OF THE URIC ACID SENSOR

To verify the FPCB sensor's durability, we fold the FPCB sensor multiple times. Fig. 11 (a) shows the UA sensor in a flat state, and Fig. 11 (b) shows the UA sensor in a curve state which shows the littlest effect on the FPCB substrate and copper wires. Also, verifying fold times in UA sensor has minimal inference on linearity and average sensitivity. We measure UA sensor fold 0 times, 100 times, and 200 times average sensitivity and linearity. Fig. 12 shows the result; the fold crease doesn't affect average sensitivity and linearity.

### I. COMPARISONS OF URIC ACID SENSORS BASED ON DIFFERENT STRUCTURES

Table 2 shows the comparisons of the sensing performances based on uric acid sensors with different structures. In this work, we had the best average sensitivity of 22.50 mV/(mg/dL) and linearity of 0.999 in the potentiometric sensor. Compared to recent research, the ERGO-modified ZnO-NSs [36] has lower LOD due to amperometry measurement and nanostructure. Identically, in Ali's study, the nanostructure of ZnO-NFs [21] and ZnO-NWs [22] can

**TABLE 2. Comparisons of the sensing performances based on uric acid sensors with different structures.**

| Working electrode structure | Sensing architecture | Average sensitivity (mV/(mg/dL)) | Linearity | Linear range (mg/dL) | LOD (μM) | Response time (seconds) | Ref. |
|---|---|---|---|---|---|---|---|
| Nafion/Uricase/ZnO | Electrochemical V-T measurement | 22.50 | 0.999 | 2 - 10 | 7.14 | 7 | This work |
| ITO- ERGO /ZnO-NSs | Amperometry | 150.7 μA $cm^{-2}$ $mM^{-1}$ | 0.997 | 0.02 – 6.72 | 0.45 | N/A | [36] 2022 |
| Uricase/$RuO_2$ | Electrochemical V-T measurement | 7.15 | 0.997 | 2 - 10 | N/A | 25 | [37] 2021 |
| Uricase/$RuO_2$ | EGFET resistive divider | 12.69 | 0.997 | 2 - 10 | 4.89 | 8 | [30] 2021 |
| Nafion/Uricase /ZnO-NFs | Electrochemical | 8.88 | 0.99 | 0.01 - 27.27 | 1 | 6-9 | [21] 2012 |
| Nafion/Uricase /ZnO-NWs | Electrochemical | 4.72 | N/A | 0.02 - 18.18 | 0.5 | 8 | [22] 2011 |

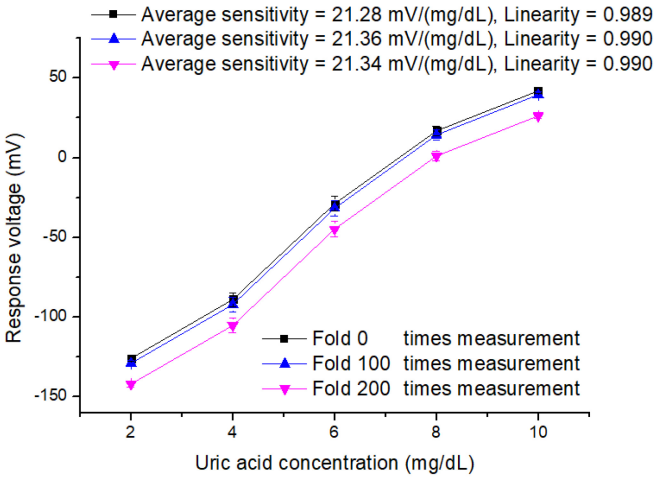


**FIGURE 12. Average UA sensitivity of the sensor versus folding times.**

achieve lower LOD but lower average sensitivity. In Kuo's study, the $RuO_2$ UA sensor can be applicated to electrochemical [37] and EGFET [30] measurement. Both studies achieve array sensing windows and can analyze multiple working electrodes simultaneously. Also, the average sensitivity seems applicable. Finally, comparing the sensor's response time, 7 second response time was fast enough compared to another potentiometric enzymatic UA sensor.

## IV. CONCLUSION

As a biosensing device, the proposed enzymatic Nafion/uricase/ZnO/ENIG/Cu/PI sensor can successfully detect uric acid. The ZnO thin films were successfully prepared by a radio frequency sputtering system and deposited on polyimide and immersion gold substrates based on FPCB standard process. In terms of enzyme immobilization, we used the APTES, uricase, glutaraldehyde cross-link technic, and Nafion was successfully applied to the uric acid sensor. The potentiometric measurement system was applied to analyze biosensor performance. For UA sensor performance, the uric acid measure concentration range of 2-10 mg/dL has 22.50 mV/(mg/dL) average sensitivity, low LOD (7.14 $\mu$M), good selectivity, and linearity was 0.999. Furthermore, we evaluate sensor reproducibility for stability concerns, and sensitivity has a standard deviation of 8.2%. Ultimately, the short response time of 7 seconds was measured.

## REFERENCES

[1] S. Jain, S. Verma, S. P. Singh, and S. N. Sharma, "An electrochemical biosensor based on novel butylamine capped CZTS nanoparticles immobilized by uricase for uric acid detection," *Biosens. Bioelectron.*, vol. 127, pp. 135–141, Feb. 2019.

[2] Y. Fu, H. Yang, and J. Guo, "Electrochemical test strip-based accurate blood uric acid measurement by adding blood cell filtration membrane," *IEEE Trans. Ind. Informat.*, vol. 15, no. 12, pp. 6389–6394, Dec. 2019.

[3] A. A. Belyustin, "The centenary of glass electrode: From Max Cremer to F. G. K. Baucke," *J. Solid-State Electrochem.*, vol. 15, no. 1, pp. 47–65, Jan. 2011.

[4] L. C. Clark Jr. and C. Lyons, "Electrode systems for continuous monitoring in cardiovascular surgery," *Ann. New York Acad. Sci.*, vol. 102, no. 1, pp. 29–45, Oct. 1962.

[5] Y.-H. Liao and J.-C. Chou, "Potentiometric multisensor based on ruthenium dioxide thin film with a Bluetooth wireless and Web-based remote measurement system," *IEEE Sensors J.*, vol. 9, no. 12, pp. 1887–1894, Dec. 2009.

[6] W. Guan, X. Duan, and M. A. Reed, "Highly specific and sensitive non-enzymatic determination of uric acid in serum and urine by extended gate field effect transistor sensors," *Biosens. Bioelectron.*, vol. 51, pp. 225–231, Jan. 2014.

[7] W. He, X. Ye, and T. Cui, "Flexible electrochemical sensor with graphene and gold nanoparticles to detect dopamine and uric acid," *IEEE Sensors J.*, vol. 21, no. 23, pp. 26556–26565, Dec. 2021.

[8] H. A. Bulger and H. E. Johns, "The determination of plasma uric acid," *J. Biol. Chem.*, vol. 140, no. 2, pp. 427–440, Aug. 1941.

[9] S. Kumar et al., "Development of uric acid biosensor using gold nanoparticles and graphene oxide functionalized micro-ball fiber sensor probe," *IEEE Trans. NanoBiosci.*, vol. 19, no. 2, pp. 173–182, Apr. 2020.

[10] L. Singh et al., "Gold nanoparticles and uricase functionalized tapered fiber sensor for uric acid detection," *IEEE Sensors J.*, vol. 20, no. 1, pp. 219–226, Jan. 2020.

[11] M. Batumalay, S. W. Harun, F. Ahmad, R. M. Nor, N. R. Zulkepely, and H. Ahmad, "Tapered plastic optical fiber coated with graphene for uric acid detection," *IEEE Sensors J.*, vol. 14, no. 5, pp. 1704–1709, May 2014.
[12] M. Verma, T. K. Naqvi, S. K. Tripathi, M. M. Kulkarni, N. E. Prasad, and P. K. Dwivedi, "Plasmonic paper-based flexible SERS biosensor for highly sensitive detection of lactic and uric acid," *IEEE Trans. NanoBiosci.*, vol. 21, no. 2, pp. 294–300, Apr. 2022.
[13] R. Kant, R. Tabassum, and B. D. Gupta, "Fiber optic SPR-based uric acid biosensor using uricase entrapped polyacrylamide gel," *IEEE Photon. Technol. Lett.*, vol. 28, no. 19, pp. 2050–2053, Oct. 1, 2016.
[14] C.-Y. Wang, C.-W. Huang, T.-T. Wei, M.-Y. Wu, and Y.-W. Lin, "Fluorescent detection of uric acid in biological samples through the inhibition of cobalt(II) catalyzed Amplex UltraRed," *Sens. Actuat. B, Chem.*, vol. 244, pp. 357–364, Jun. 2017.
[15] P.-H. Yang, C.-T. Chan, and Y.-S. Zhang, "ZnO film flexible printed circuit board pH sensor measurement and characterization," *IEEE Access*, vol. 10, pp. 96091–96099, 2022.
[16] C. J. Freeman, B. Ullah, M. S. Islam, and M. M. Collinson, "Potentiometric biosensing of ascorbic acid, uric acid, and cysteine in microliter volumes using miniaturized nanoporous gold electrodes," *Biosensors*, vol. 11, no. 1, p. 10, Dec. 2020.
[17] S. Critcher and T. J. Freeborn, "Flexible PCB failures from dynamic activity and their impacts on bioimpedance measurements: A wearable case study," *IEEE Open J. Circuits Syst.*, vol. 2, pp. 732–742, 2021.
[18] J.-C. Chou et al., "Increasing the photovoltaic performance of dye-sensitized solar cells by zinc oxide film as a recombination blocking layer," *IEEE Trans. Electron Devices*, vol. 69, no. 9, pp. 5004–5011, Sep. 2022.
[19] R. S. Singh and K. Chauhan, "Immobilization of inulinase on aminated multiwalled carbon nanotubes by glutaraldehyde cross-linking for the production of fructose," *Catalysis Lett.*, vol. 149, no. 10, pp. 2718–2727, Oct. 2019.
[20] Y. J. Lee, D. J. Park, and J. Y. Park, "Fully packaged nonenzymatic glucose microsensors with nanoporous platinum electrodes for anti-fouling," *IEEE Sensors J.*, vol. 8, no. 11, pp. 1922–1927, Nov. 2008.
[21] S. M. U. Ali, Z. H. Ibupoto, M. Kashif, U. Hashim, and M. Willander, "A potentiometric indirect uric acid sensor based on ZnO nanoflakes and immobilized uricase," *Sensors*, vol. 12, no. 3, pp. 2787–2797, Mar. 2012.
[22] S. M. U. Ali, N. H. Alvi, Z. Ibupoto, O. Nur, M. Willander, and B. Danielsson, "Selective potentiometric determination of uric acid with uricase immobilized on ZnO nanowires," *Sens. Actuat. B, Chem.*, vol. 152, no. 2, pp. 241–247, Mar. 2011.
[23] E. Martynenko, W. Zhou, A. Chudnovsky, R. S. Li, and L. Poglitsch, "High cycle fatigue resistance and reliability assessment of flexible printed circuitry," *J. Electron. Packag.*, vol. 124, pp. 254–259, Sep. 2002.
[24] "Single resistor gain programmable, precision instrumentation amplifier," Data Sheet LT1167, Linear Technol., Milpitas, CA, USA, Aug. 2011.
[25] Y.-H. Liao and J.-C. Chou, "Weighted data fusion use for ruthenium dioxide thin film pH array electrodes," *IEEE Sensors J.*, vol. 9, no. 7, pp. 842–848, Jul. 2009.
[26] K.-H. Bang, D.-K. Hwang, and J.-M. Myoung, "Effects of ZnO buffer layer thickness on properties of ZnO thin films deposited by radio-frequency magnetron sputtering," *Appl. Surface Sci.*, vol. 207, nos. 1–4, pp. 359–364, Feb. 2003.
[27] M. N. Islam, T. B. Ghosh, K. L. Chopra, and H. N. Acharya, "XPS and X-ray diffraction studies of aluminum-doped zinc oxide transparent conducting films," *Thin Solid Films*, vol. 280, nos. 1–2, pp. 20–25, Jul. 1996.
[28] D. Park, Y. Yang, and K. Kim, "Evaluation of the mechanical properties of ZnO nanorods treated with oxygen plasma using atomic force microscopy," *Korean J. Metals Mater.*, vol. 59, no. 3, pp. 209–216, Feb. 2021.
[29] T. K. Le et al., "Formation of surface defects by thermal shock method for the improved photocatalytic activity of ZnO nanoparticles," *J. Asian Ceram. Soc.*, vol. 8, no. 1, pp. 193–202, Jan. 2020.
[30] P.-Y. Kuo, Y.-Y. Chen, W.-H. Lai, and C.-H. Chang, "An extended-gate field-effect transistor applied to resistive divider integrated with the readout circuit using 180nm CMOS process for uric acid detection," *IEEE Sensors J.*, vol. 21, no. 18, pp. 20229–20238, Sep. 2021.
[31] H. Santha, R. Dobay, and G. Harsanyi, "Amperometric uric acid biosensors fabricated of various types of uricase enzymes," *IEEE Sensors J.*, vol. 3, no. 3, pp. 282–287, Jun. 2003.
[32] N. Bhalla, P. Jolly, N. Formisano, and P. Estrela, "Introduction to biosensors," *Essays Biochem.*, vol. 60, no. 1, pp. 1–8, 2016.
[33] D. Feng, F. Wang, and Z. Chen, "Electrochemical glucose sensor based on one-step construction of gold nanoparticle–chitosan composite film," *Sens. Actuat. B, Chem.*, vol. 138, no. 2, pp. 539–544, May 2009.
[34] J.-C. Chou et al., "Study of the glucose sensor based on potentiometric non-enzymatic Nafion/CZO thin film," *IEEE Sensors J.*, vol. 21, no. 14, pp. 15926–15934, Jul. 2021.
[35] J.-C. Chou et al., "Characteristics and stability of a flexible arrayed uric acid biosensor based on NiO film modified by graphene and magnetic beads," *IEEE Sensors J.*, vol. 21, no. 6, pp. 7218–7225, Mar. 2021.
[36] M. Eryiğit, B. K. Urhan, H. Ö. Doğan, T. Ö. Özer, and Ü. Demir, "ZnO nanosheets-decorated ERGO layers: An efficient electrochemical sensor for non-enzymatic uric acid detection," *IEEE Sensors J.*, vol. 22, no. 6, pp. 5555–5561, Mar. 2022.
[37] P. Y. Kuo and Y. Y. Chen, "A novel low unity-gain frequency and low power consumption instrumentation amplifier design for $RuO_2$ uric acid biosensor measurement," *IEEE Trans. Instrum. Meas.*, vol. 70, pp. 1–9, 2021.

**PO-HUI YANG** (Member, IEEE) was born in Tainan, Taiwan, in 1965. He received the B.Eng. degree in marine electronics engineering from National Taiwan Ocean University, Keelung, Taiwan, in 1993, the M.S. degree in industrial education from National Taiwan Normal University, Taipei, Taiwan, in 1995, and the Ph.D. degree from the Institute of Electrical Engineering, National Chung Cheng University, Chiayi, Taiwan, in 2001. From 2001 to 2003, he was an Assistant Professor with the Department of Electronics, Southern Taiwan University of Science and Technology. From 2003 to 2004, he was a High-Performance Digital IC Design Engineer and a Circuit Design Section Manager with the SoC Technology Center, Industrial Technology Research Institute, Hsinchu, Taiwan. In 2004, he joined the Department of Electronic Engineering, National Yunlin University of Science and Technology, where he is currently an Associate Professor. His research interests include high-speed and low-power CMOS IC design, advanced IC packaging, and low-power biosensor IC design.

**CHE-TSUNG CHAN** was born in Taichung, Taiwan, in November 1998. He received the bachelor's degree from the Department of Electronic Engineering, National Yunlin University of Science and Technology, Yunlin, Taiwan, in 2020, where he is currently pursuing the master's degree with the Graduate School of Electronic Engineering. His research interests include analog circuits for biosensors and digital glitch cancellation circuits.

**YING-SHENG CHANG** was born in Taoyuan, Taiwan, in February 1999. He received the bachelor's degree from the Department of Electronic Engineering, National Yunlin University of Science and Technology, Yunlin, Taiwan, in 2020, where he is currently pursuing the master's degree with the Graduate School of Electronic Engineering. His research interests include analog readout circuits and temperature compensation circuits for biosensors measurement systems.